Identification of the mechanism of NO reduction with ammonia (SCR) on zeolite catalysts

Authors: Konstantin Khivantsev,[1,†,*] Ja-Hun Kwak,[2,†,*] Nicholas R. Jaegers,[1] Miroslaw A. Derewinski,[1,3] Janos Szanyi,[1,†,*]

Affiliations:

[1] Institute for Integrated Catalysis, Pacific Northwest National Laboratory, Richland, WA 99352, USA.

[2] Ulsan National Institute of Science and Technology (UNIST), South Korea.

[3] Jerzy Haber Institute of Catalysis and Surface Chemistry, Polish Academy of Sciences, Krakow 30-239, Poland

* Correspondence to: K.K. E-mail: Konstantin.Khivantsev@pnnl.gov . J.-H. K. E-mail: jhkwak@unist.ac.kr . J.Sz. E-mail: Janos.Szanyi@pnnl.gov;

† These authors contributed equally to the manuscript: KK, JHK, JSz

Short title: Clarification of the selective catalytic reduction mechanism

Abstract: Cu/Zeolites catalyze selective catalytic reduction of nitric oxide with ammonia. Although the progress has been made in understanding the rate-limiting step of reaction which is reoxidation of $Cu(I)(NH_3)_2$ with oxygen to restore the catalytically active Cu(II) site, the exact NO reduction chemistry remained unknown. Herein, we show that nitrosyl ions NO^+ in the zeolitic micropores are the true active sites for NO reduction. They react with ammonia even at below/room temperature producing molecular nitrogen through the intermediacy of N_2H^+ cation. Isotopic experiments confirm our findings. No copper is needed for this reaction to occur. However, when NO^+ reacts, "freed up" Bronsted acid site gets occupied by NH_3 to form NH_4^+ – and so the catalytic cycle stops because NO^+ does not form on NH_4-Zeolites due to their acid sites being already occupied. Therefore, the role of Cu(II) in Cu/Zeolite catalysts is to produce NO^+ by the reaction: $Cu(II) + NO \rightarrow Cu(I) + NO^+$ which we further confirm spectroscopically. The NO^+ then reacts with ammonia to produce nitrogen and water. Furthermore, when Cu(I) gets re-oxidized the catalytic cycle then can continue. Thus, our findings are critical for understanding complete SCR mechanism.

One Sentence Summary: We clarify the long-standing unknown SCR mechanism.

Air pollution is one of the main health and environmental concerns in our (post)industrial society [1-3]. Worsening air quality is tied to toxic nitric oxide (NO) gas, the majority of which is emitted by vehicles exhaust. The ability of Cu/zeolites to scrub NO in the presence of ammonia was first discovered in Japan in the 1960s [4] for Cu/FAU zeolite. However, FAU framework is less stable

that the corresponding SSZ-13 and BEA zeolites [5]. Within the last decade, the ammonia selective catalytic reduction (SCR) technology was implemented on the large scale [5-19] for diesel engines on the basis of Cu(Fe) in BEA and SSZ-13 zeolites.

Remarkable advances have been achieved towards the goal of understanding the rate-limiting steps of the SCR mechanism [5-20]. Cu(II) ions are present in Cu/zeolite materials (they were shown to be more active and hydrothermally stable than Cu(II)-OH ions [5-20,25]. The rate-limiting step for low-temperature SCR was shown to be re-oxidation of reduced $Cu(I)(NH_3)_2$ complexes via the formation of transient $(NH_3)_2Cu(II)-O_2-Cu(II)(NH_3)_2$ dimers [17,18]. Despite that, the mechanism of the steps involving NO reduction with NH_3 remained largely unknown [5-20].

We selectively formed NO^+ ion in H-BEA zeolite (typical helium ion images of H-BEA are shown in Fig. S6) by reaction of NO with sub-stoichiometric amounts of O_2 [21-23](Fig. 1A).

NO^+ is formed through the following reaction (**Scheme 1** responsible for spectra in Fig 1A):

$$2NO + 1/2O_2 + 2 \text{ H-Zeolite} \rightarrow 2NO^+ + H_2O$$

NO^+ occupies two different cationic positions with the corresponding N-O stretching frequencies at ~2133 and ~2175 cm^{-1}. The same type of chemistry also occurs on H-SSZ-13 (Fig. S1). Please note that adsorption of NO_2 also produces NO^+ but with stoichiometric NO_3^- amounts due to N_2O_4 disproportionation (Fig. S2). Pulling the high vacuum (~10^{-7} Torr) (with quick heating to 150 °C) allows to remove excessive NO and O_2, leaving zeolite with NO^+ adsorbed in it (Fig. 1B).
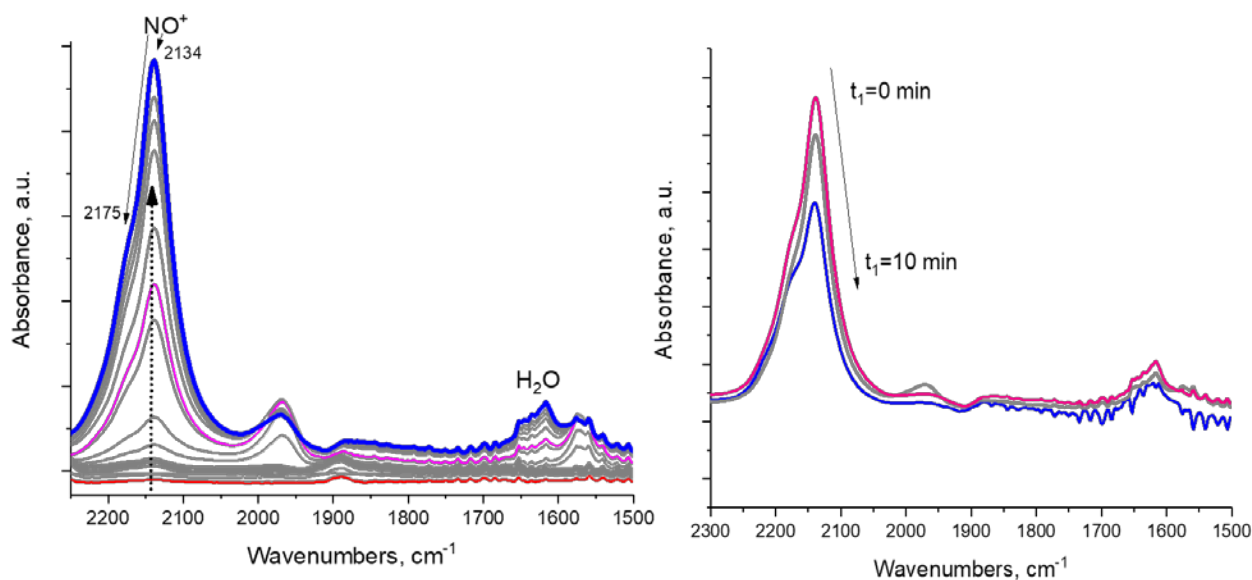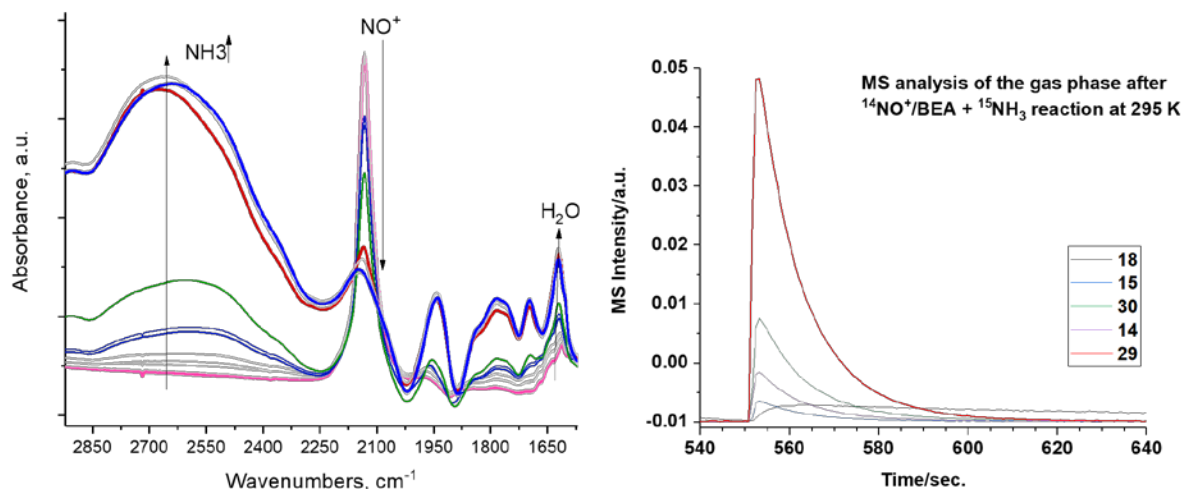
Fig.1 H-BEA Zeolite with Si/Al ~ 15. **A (left spectrum)**: *in-situ* FTIR during first sequential NO adsorption (0.1 Torr equilibrium pressure), followed by sequential O_2 addition (0.17 Torr total eq. pressure – when O_2 is added, NO^+ begins to develop in significant amounts); **B (right spectrum)**: FTIR after pulling high vacuum 10^{-8} Torr from time=0 to time=10 minutes at 150 °C. Spectra were recorded after cooling back to 297 K.

We exposed the NO^+/Zeolite to ^{15}N-labeled ammonia at room temperature 297 K (Fig. 2A). Ammonia first occupies Bronsted acid sites forming NH_4^+ complexes (which interact with more NH_3 and the pores are filled with $(NH_3)x$ cluster networks interacting with NH_4^+ ions [24,27]). During this, NO^+ reacts with ammonia, leaving no new visible NO stretches (Fig. 2A).
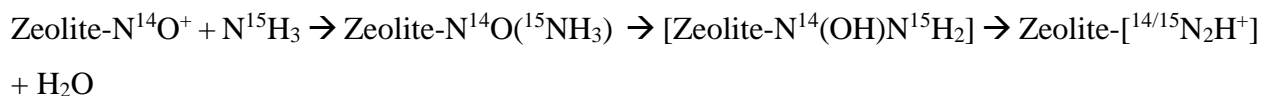

Fig. 2. H-BEA zeolite with Si/Al~15. **A (left spectrum)**: *in-situ* sequential FTIR during [15]NH3 adsorption (total equilibrium pressure 0.020 Torr) on NO^+/H-BEA sample at room temperature. Ammonia reacts with NO^+. Gas phase from that reaction was analyzed with the mass spectrometer attached to the IR cell (**Figure 2B** shows formation of [14]N[15]N dinitrogen with the characteristic 29 mass signal).
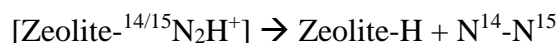
The analysis of the gas-phase product with mass-spectrometry reveals a major peak at 29, corresponding to [14]N-^{15}N molecules (Fig. 2B). Thus, NO^+ reacts with ammonia with the formation of molecular nitrogen already at room temperature. Only the following sequence can be envisioned (**Schemes 2 and 3**) (note that NO^+ does not necessarily have to be bound to zeolite, it most likely is solvated by NH_3; the designation Zeolite-NO^+ is just a representation of NO^+/H-zeolite system in which NO^+ may be solvated or semi-solvated by ammonia molecules):

Zeolite-N[14]O$^+$ + N[15]H$_3$ → Zeolite-N[14]O([15]NH$_3$) → [Zeolite-N[14](OH)N[15]H$_2$] → Zeolite-[[14/15]N$_2$H$^+$] + H$_2$O

[Zeolite-[14/15]N$_2$H$^+$] → Zeolite-H + N[14]-N[15]

N_2H^+ (hydronium diazonium cation) is extremely unstable. Its immediate decomposition to N_2 and H-Zeolite is what drives this reaction. Despite that, we find that at sufficiently high molecular N_2 pressure in the cell (~15Torr) we can observe the N-N stretch of $-HN_2^+$ complex at 2334 cm^{-1} even at room temperature (Fig 3A), which was previously shown to form only at low temperatures upon N_2 interaction with Bronsted acid sites (Fig. 3B) [26]. Thus, we can observe the intermediate of this reaction indirectly.
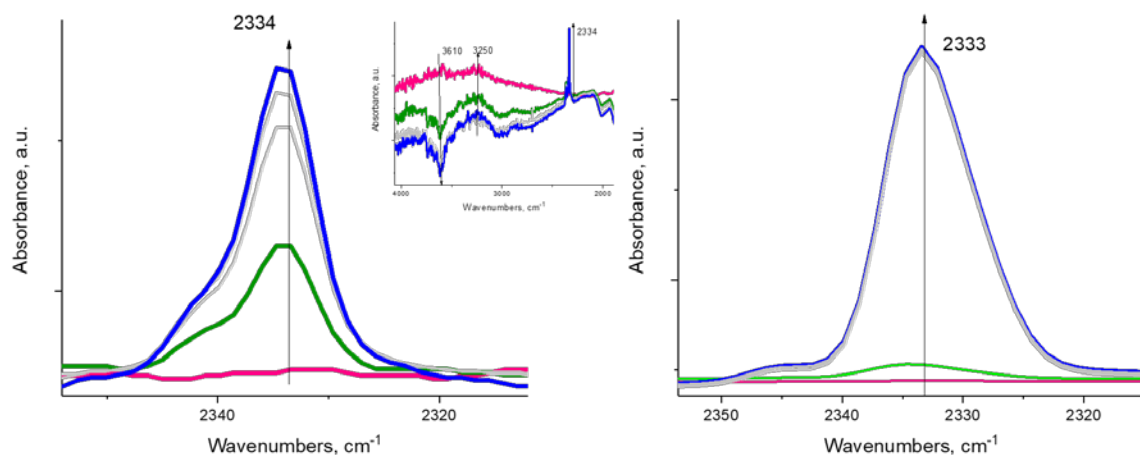
Fig. 3. **A (left spectrum)**: *in-situ* FTIR during sequential dinitrogen N_2 adsorption (equilibrium pressure ~15 Torr) on H-BEA at 298 K. Zeolite-[HN_2^+] complex can be observed even at room temperature. Inset shows that N_2 interacts with Bronsted acid sites of Si-OH-Al zeolite groups (OH stretch of such groups is located at ~3610 cm^{-1}). **B(right spectrum)**: *in-situ* FTIR during Adsorption of only ~0.1 Torr N_2 on the same H-BEA tablet (equilibrium pressure is 0.001 Torr) at 77 K produces N-N stretches of N_2 adsorbed on Bronsted acid sites. Note that in this case even low equilibrium pressure of nitrogen produces intense N-N stretches.

To further prove the reaction proceeds through diazo compound, we chose aniline $PhNH_2$ (which is equivalent to ammonia molecule but with 1 hydrogen atom substituted by a phenyl group) and reacted it with NO^+ in BEA zeolite. Phenyl group stabilizes the formation of PhN_2^+ salts (phenyl diazonium salts) through the mesomeric effect, and thus, unlike alkyl diazonium salts, aryl diazonium compounds are stable and characterized by N-N stretches in ~2,250-2,300 cm^{-1} region [28], more specifically ~2,280 cm^{-1} for phenyl diazonium in solution [28]. Indeed, we monitored the reaction of NO^+ and $PhNH_2$, spectroscopically: NO^+ band went down and a new N-N stretch appeared at ~2270 cm^{-1}, corresponding to the N-N vibration of Ph-N_2^+ fragment (Fig. 4).

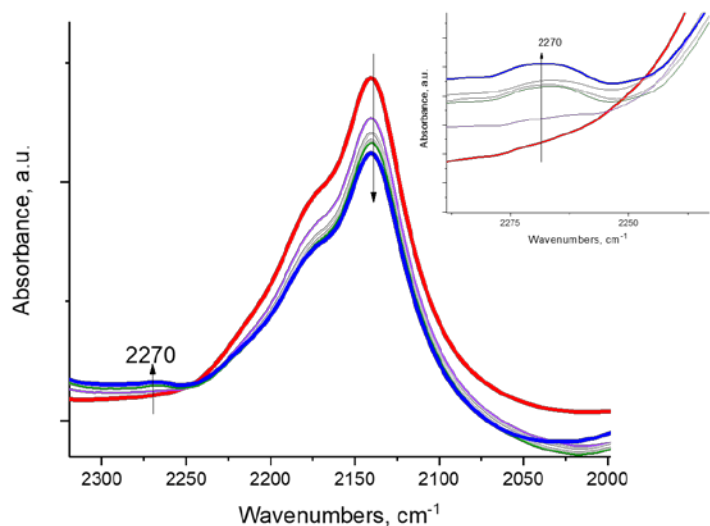Fig. 4. *in-situ* FTIR during sequential ~0.3 Torr aniline PhNH$_2$ adsorption (equilibrium pressure ~0.03 Torr) NO$^+$/H-BEA.

NO$^+$ in H-SSZ-13 (with Si/Al ~12; typical HAADF-STEM images of this sample are shown in Fig. S7) similarly reacts to NH$_3$ (Fig. 5), with concomitant N$_2$ evolution (confirmed with mass-spectrometry):
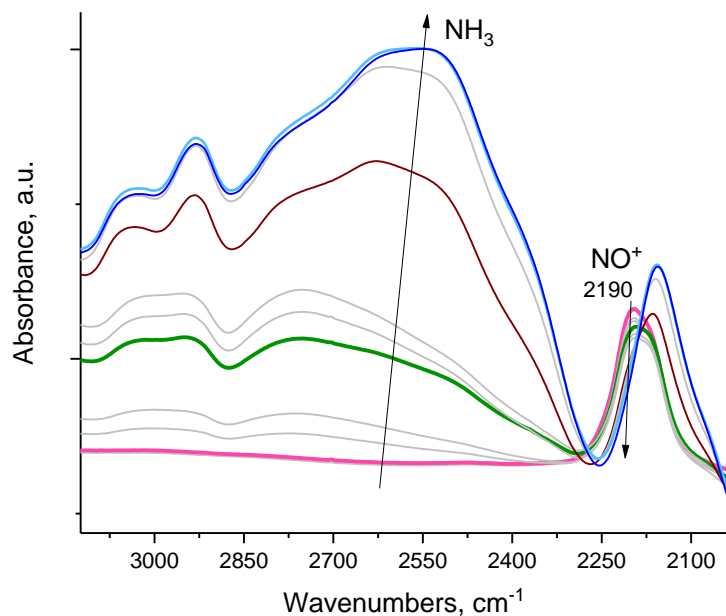

Fig. 5. H-SSZ-13 zeolite with Si/Al~12. In-situ sequential FTIR during ^{14}NH$_3$ adsorption (total equilibrium pressure ~0.15 Torr) on NO$^+$/H-SSZ-13 sample at room temperature. Ammonia reacts with NO$^+$ as evidenced by the disappearance of NO$^+$ stretch. The intense band at ~ 2110 cm^{-1} is due to zeolite interactions with NH$_3$. Pulling vacuum on the sample at 120 ºC produces spectra showing no NO$^+$ stretches (Fig. S3), consistent with complete reaction of NO$^+$.

Thus, NO^+ (which is produced from $NO+O_2$ reaction/it can also form from N_2O_4 disproportionation on zeolites if sufficient NO_2 concentration is present [29]) is the critical intermediate in conversion of NO on zeolites. *Copper is not even required to observe the NO^+ reduction by NH_3.*

Moreover, we reacted inorganic nitrosyl salt NO^+ with $^{15}NH_3$ and observed ^{14}N-^{15}N in the gas-phase (consistent with our findings for NO^+ in zeolites, *this reaction takes place vigorously even at temperatures as low -50 ⁰C*) (**Scheme 4**):

$^{14}NO[BF_4] + {}^{15}NH_3$ (at -50 ⁰C)$\rightarrow {}^{14}N^{15}N$ (gas) $+ H_2O + H[BF_4]$
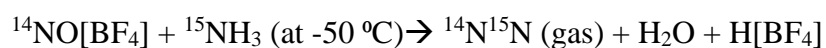
This reaction (**scheme 4**) most likely proceeds through N_2H^+ intermediate as well.

For NO^+ in zeolite, once it reacts with NH_3 with the release of N_2, the Bronsted acid is freed up from NO^+ and then immediately occupied by ammonia with the formation of NH_4^+. This "kills" the reactivity as we cannot produce NO^+ species anymore since their production requires Bronsted acid sites, as evidenced by FTIR (Fig. S4): indeed, no NO^+ evolves in above-trace-amount upon $NO+O_2$ reaction on NH_4-zeolite (Fig. S4). Only at elevated temperature, when some NH_3 can desorb and free up a portion of Bronsted acid sites to re-form NO^+, the reaction can proceed catalytically. Indeed, bare H-BEA zeolite is catalytically active for NO reduction with NH_3 in the dry streams (see Fig. S5 for reactivity at 200 and 150 ⁰C with time-on-stream) (measurable activity is observed).

NO^+ are formed in zeolite through **Scheme 1** (see earlier discussion in the manuscript).

With these new data, we can finally explain the role of Cu in zeolites for SCR. As is well-established in the literature, Cu(II) ions are required for the active continuous catalytic reaction to proceed [5-20]. In the presence of NO, Cu(II) ions can produce NO^+ via the formal 1-electron reduction of Cu(II) (analogous chemistry is observed, for example, for Pd(II) in zeolites [30] where Pd(II) was shown to be reduced to Pd(I) by NO pulse with concomitant formation of NO^+) (**Scheme 5**):

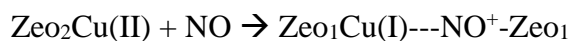$Zeo_2Cu(II) + NO \rightarrow Zeo_1Cu(I)$---$NO^+$-$Zeo_1$

Fig. 6A shows spectroscopic evidence of Cu(II) reduction by NO (when Cu(II) is first reduced to Cu(I) before NO adsorption, basically very little NO$^+$ formation occurs because electron transfer does not take place as demonstrated in Fig 6B).
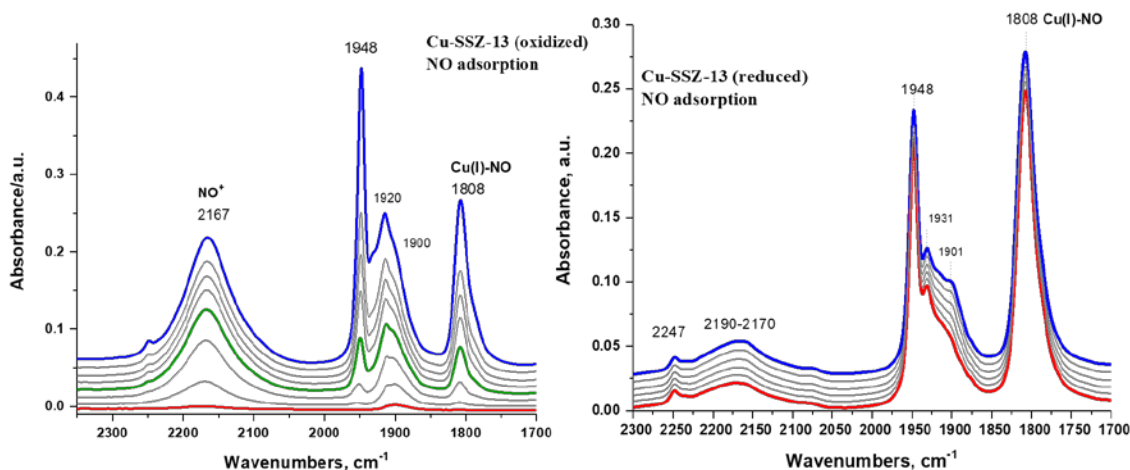

Fig. 5. 1 wt% Cu/H-SSZ-13 sample with Si/Al ~ 12. **A(left)**: in-situ FTIR during 1 Torr NO adsorption on oxidized sample. NO$^+$ and Cu(I)-NO evolve simultaneously from Cu(II) reduction by NO. **B(right)**: the same sample (tablet) was reduced in the IR cell: 1 Torr NO adsorption (same equilibrium pressure) after reduction.

We have previously been able to refine with solid-state ^{15}NMR studies that ,indeed, NO is capable of reducing Cu(II) to Cu(I) in H-SSZ-13: the resulting complex had Cu(I) and NO$^+$ in proximity to each other, with NO$^+$ located side-on towards copper ion [20].

Therefore, now we conclude that the role of copper is to promote NO$^+$ formation (because Bronsted acid sites get occupied by NH$_4^+$ after NO$^+$ reaction with NH$_3$ on bare H-Zeolite, they cannot contribute to NO$^+$ formation as we showed earlier in the text). The resulting NO$^+$ reacts with ammonia to reform N$_2$. The Cu(I)(NH$_3$)$_2$ complex, in turn, gets re-oxidized back to Cu(II) with oxygen as the rate-limiting step [17,18].

In summary, this study resolves the previously missing chemistry of the SCR reaction on zeolitic materials and explains the role of Cu for SCR. For the first time, NO$^+$ is shown to be the crucial reactive intermediate without which the reaction cannot proceed. The catalytic reaction is suggested to proceed through the formation of previously unrecognized diazo-complex N$_2$H$^+$. The role of copper is to be a redox active center which facilitates the formation of NO$^+$ from NO while

simultaneously getting reduced to Cu(I). During the rate-limiting step, Cu(I) gets re-oxidized by O$_2$ to Cu(II), thus completing the catalytic cycle.

References

(1) Royal College of Paediatrics and Child Health . Every breath we take—the lifelong impact of air pollution. London: Royal College of Paediatrics and Child Health, 2016.

(2) Sachtler W.M.H. (2002) Catalysis from Art to Science. In: Carley A.F., Davies P.R., Hutchings G.J., Spencer M.S. (eds) Surface Chemistry and Catalysis. Fundamental and Applied Catalysis. Springer, Boston, MA

(3) Khair, M. K.; Majewski, W. A. Diesel emissions and their control; SAE International, Warrendale, 2006.

(4) T. Seiyama, T. Arakawa, T. Matsuda, N. Yamazoe, and Y. Takita, Chem. Lett., 781 (1975)

(5) Zones, S.I. US Patent 4 544 538, 1985.

(6) Ja-Hun Kwak, Russell G Tonkyn, Do Heui Kim, János Szanyi, Charles HF Peden, J. Catal., 2010, 275, 187-190.

(7) I. Bull, A. Moini, G. Koermer, J. Patchett, W. Jaglowski, S. Roth, US Patent US20070134146A1, 2010.

(8) DW Fickel, RF Lobo, The Journal of Physical Chemistry C, 2010, 114 (3), 1633-1640.

(9) J.H. Kwak, D. Tran, S.D. Burton, J. Szanyi, J.H. Lee, C.H.F. Peden J. Catal., 287 (2012), p. 203.

(10) J.H. Kwak, D. Tran, J. Szanyi, C.H.F. Peden, J.H. Lee, Catal. Lett., 142 (2012), p. 295.

(11) S.J. Schmieg, S.H. Oh, C.H. Kim, D.B. Brown, J.H. Lee, C.H.F. Peden, D.H. Kim, Catal. Today, 184 (2012), p. 252.

(12) J.H. Kwak, H.Y. Zhu, J.H. Lee, C.H.F. Peden, J. Szanyi, Chem. Commun., 48 (2012), p. 4758.

(13) F. Gao, J. H. Kwak, J. Szanyi and C. H. F. Peden, Top. Catal., 2013, 56, 1441–1459.

(14) ST Korhonen, DW Fickel, RF Lobo, BM Weckhuysen, AM Beale, Chemical Communications 47 (2), 800-802

(15) F. Gao, E. D. Walter, E. M. Karp, J. Y. Luo, R. G. Tonkyn, J. H. Kwak, J. Szanyi and C. H. F. Peden, J. Catal., 2013, 300, 20–29.

(16) J. H. Kwak, T. Varga, C. H. F. Peden, F. Gao, J. C. Hanson and J. Szanyi, J. Catal., 2014, 314, 83–93.

(17) Gao, F.; Mei, D. H.; Wang, Y. L.; Szanyi, J.; Peden, C. H. F. J. Am. Chem. Soc. 2017, 139, 4935–4942.

(18) Gao, F.; Walter, E. D.; Kollar, M.; Wang, Y.; Szanyi, J.; Peden, C. H. F. J. Catal. 2014, 319, 1–14.

(19) Beale, A. M.; Gao, F.; Lezcano-Gonzalez, I.; Peden, C. H. F.; Szanyi, J. Chem. Soc. Rev. 2015, 44, 7371–7405.

(20) Kwak, J. H.; Lee, J. H.; Burton, S. D.; Lipton, A. S.; Peden, C. H. F.; Szanyi, J., Angew. Chem. Int. Ed. 2013, 52, 9985–9989.

(21) Hadjiivanov, K. I., Catal. Rev. Sci. Eng. 2000, 42, 71-144.

(22) Hadjiivanov, K.; Saussey, J.; Freysz, J. L.; Lavalley, J. C., Catal. Lett. 1998, 52, 103–108.

(23) Szanyi, J.; Paffett, M. T., J. Catal. 1996, 164, 232–245.

(24) A. Zecchina, L. Marchese, S. Bordiga, C. Paze, E. Gianotti, J. Phys. Chem. B, 101 (1997), p. 10128

(25) Negri, C.; Selleri, T.; Borfecchia, E.; Martini, A.; Lomachenko, K. A.; Janssens, T. V.W.; Cutini, M.; Bordiga, S.; Berlier, G. J. Am. Chem. Soc. 2020, 142, 15884–15896.

(26) K. Chakarova, K. Hadjiivanov, J. Phys. Chem. C, 115 (2011), p. 4806

(27) D. Perra, N. Drenchev, K. Chakarova, M.G. Cutrufello, K. Hadjiivanov, RSC Adv., 4 (2014), pp. 56183-56187.

(28) Kazitsyna L. A., Kikot B. S., and Reutov O. A. Bull. Acad. Sci. USSR, Div. Chem. Sci. (Engl. Transl.) 1964, 13, 894.

(29) J Szanyi, JH Kwak, CHF Peden, The Journal of Physical Chemistry B 108 (12), 3746-3753.

(30) Khivantsev, K.; Jaegers, N. R.; Koleva, I. Z.; Aleksandrov, H. A.; Kovarik, L.; Engelhard, M.; Gao, F.; Wang, Y.; Vayssilov, G. N.; Szanyi, J. J. Phys. Chem. C 2020, 124 (1), 309–321.

Acknowledgments:

Author contributions: All authors participated in the planning of experiments, data collection and analysis, and writing of the manuscript.

Competing interests: Authors have no conflicts to eclair.

Data and materials availability: All data is available in the main text or the supplementary materials.

Identification of the mechanism of NO reduction with ammonia (SCR) on zeolite catalysts

Authors: Konstantin Khivantsev,[1,†,*] Ja-Hun Kwak,[2,†,*] Nicholas R. Jaegers,[1] Miroslaw A. Derewinski,[1,3] Janos Szanyi,[1,†,*]

Affiliations:

[1] Institute for Integrated Catalysis, Pacific Northwest National Laboratory, Richland, WA 99352, USA.

[2] Ulsan National Institute of Science and Technology (UNIST), South Korea.

[3] Jerzy Haber Institute of Catalysis and Surface Chemistry, Polish Academy of Sciences, Krakow 30-239, Poland

* Correspondence to: K.K. E-mail: Konstantin.Khivantsev@pnnl.gov . J.-H. K. E-mail: jhkwak@unist.ac.kr . J.Sz. E-mail: Janos.Szanyi@pnnl.gov;

† These authors contributed equally to the manuscript: KK, JHK, JSz

Materials and methods

BEA with Si/Al ratio ~ 15 was synthesized in the presence of fluoride anions according to a procedure developed by Camblor et al. [S1] The gel composition was as follows SiO_2: xAl_2O_3:$(0.54+2x)$TEAOH:$(0.54+2x)$HF:$(7+2x)H_2O$. The absence of alkali cations requires only a calcination step (550 ºC in flowing air), decomposing the organic cation (TEA$^+$) to convert it into Brønsted acidic H-Form.

Na/SSZ-13 zeolite with Si/Al 12 was hydrothermally synthesized using the following recipe: 0.8 g of NaOH (Sigma Aldrich, ≥ 99%) was dissolved in 50 ml of deionized water. 17 g of TMAda-OH (Sachem Inc., 25% N,N,N-trimethyl-1-adamantyl ammonium hydroxide) was added as structure directing agent. 0.75 g of Al(OH)$_3$ (Sigma Aldrich, ~54% Al$_2$O$_3$) was slowly added to the solution and stirred at 400 rpm until it was completely dissolved. 20.0 g of LUDOX HS-30 colloidal silica (Sigma Aldrich, 30 wt% suspension in H$_2$O) was added slowly to the solution until a uniform gel was formed. The obtained gel was sealed in a 125 mL Teflon-lined stainless steel autoclave with a magnetic stirring

bar. Hydrothermal synthesis was carried out at 160 °C under continuous stirring at 400 rpm for 4 days. After synthesis, the zeolite cake was separated from the suspension by centrifugation, and washed with deionized water. It was then dried at 80 °C under N_2 flow overnight, and calcined in air at 550 °C for 5 h in order to remove the SDA. NH_4/SSZ-13 was obtained by ion exchange of the as-prepared Na/SSZ-13 zeolite with 1 M NH_4NO_3 solution at 80 °C for 5 h. The process was repeated three times. H-form of zeolite was obtained by calcining in air at 550 ºC for 5 hours. Ion-exchange with Cu(II) to produce Cu/SSZ-13 was performed in the presence of copper nitrate. The resulting sample was calcined at 550 ºC in air.

NO[BF_4] nitrosyl tetrafluoroborate (99%) was purchased from Strem Chemicals and stored cold in the absence of moisture.

All the chemicals used were the highest-grade purity available.

HAADF-STEM analysis was performed with a FEI Titan 80–300 microscope operated at 300 kV. The instrument is equipped with a CEOS GmbH double-hexapole aberration corrector for the probe-forming lens, which allows for imaging with 0.1 nm resolution in scanning transmission electron microscopy mode (STEM). The images were acquired with a high angle annular dark field (HAADF) detector with inner collection angle set to 52 mrad.

Helium ion microscopy (HIM) images were obtained using 35 keV He ions with 0.1 pA beam current at normal incidence. Secondary electrons were detected using an Everhart–Thornley detector. For HIM imaging, a very thin layer of carbon (<1 nm) was coated using a carbon sputter deposition system as the samples were completely insulating. The instrument resolution was 0.35 nm.

The *in-situ* static transmission IR experiments were conducted in a home-built cell housed in the sample compartment of a Bruker Vertex 80 spectrometer, equipped with an MCT detector and operated at 4 cm^{-1} resolution. Mass-spectrometer is attached to the cell to monitor different gaseous species present. The powder sample was pressed onto a tungsten mesh which, in turn, was mounted onto a copper heating assembly attached to a ceramic feedthrough. The sample could be resistively heated, and the sample temperature was monitored by a thermocouple spot welded onto the top center of the W grid. The cold finger on the glass bulb containing CO (99.995%) was cooled with liquid nitrogen to eliminate any contamination originating from metal carbonyls, while NO (99.95%) was cleaned with multiple freeze–pump–thaw cycles. $^{15}NH_3$ (15N, 98%) was purchased from Cambridge Isotopes. Special research-grade oxygen (purity 99.995%) was purchased from Oxarc.

The NO reduction by ammonia (in the presence of oxygen) was carried out in a typical quartz the plug-flow reactor. 120 mg of H-zeolites was used for reaction tests. The composition of the gas flowing through the catalyst was ~ 360 ppm NH_3, 360 ppm NO, ~12 % O_2 balanced with nitrogen. The total flow rate was ~ 300 sscm/min. Concentrations of reactants and products were measured by the MKS FTIR analyzer.

<u>References</u>: **S1** M.A. Camblor, A. Corma, S. Valencia Synthesis in fluoride media and characterisation of aluminosilicate zeolite beta, J. Mater. Chem., 8 (1998), pp. 2137-2145
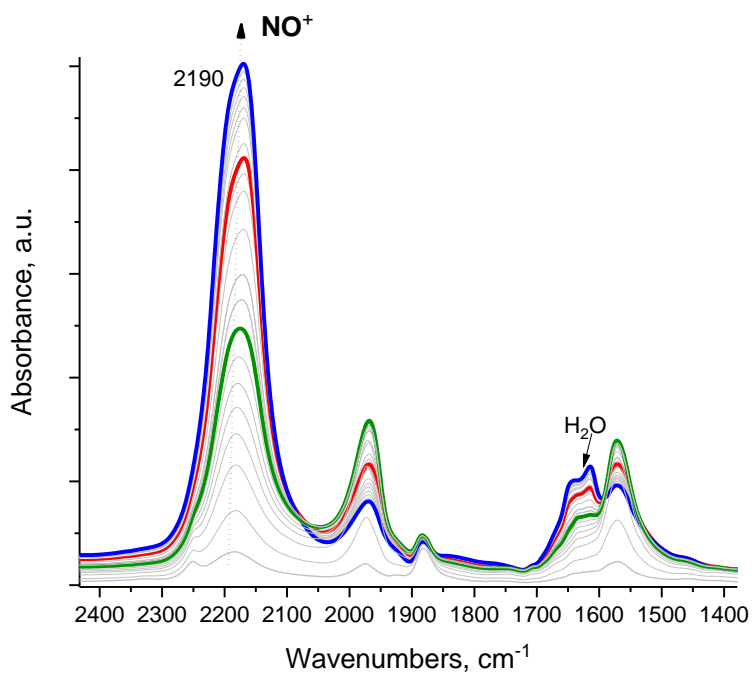
Fig. S1. *In-situ* FTIR during sequential NO (0.5 Torr) and O_2 (0.1 Torr) co-adsorption on H-SSZ-13 with Si/Al~12 at room temperature.
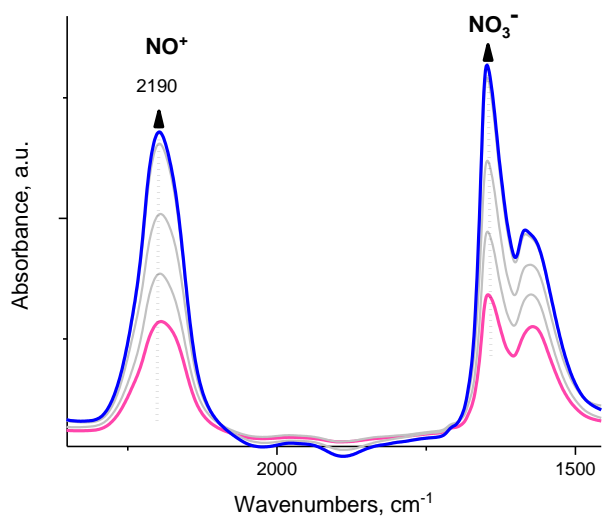

Fig. S2. *In-situ* FTIR during sequential NO_2 (0.5 Torr) on H-SSZ-13 with Si/Al~12 at room temperature. NO_2 forms N_2O_4 in the pores and immediately reacts with H-SSZ-13 to form NO^+ and HNO_3.
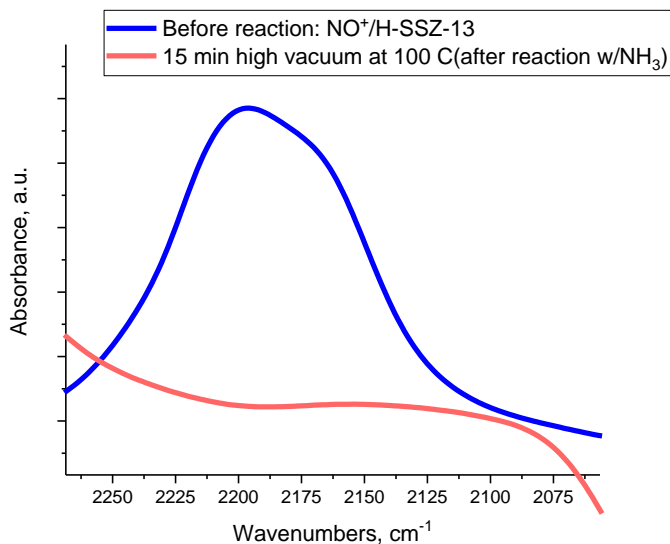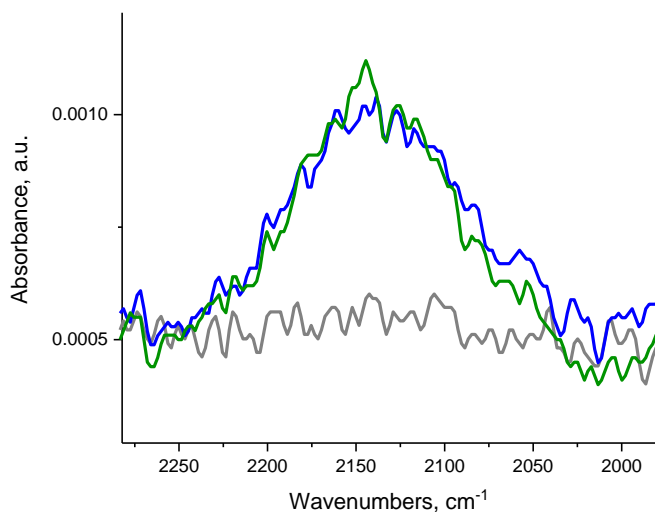
Fig. S3. *Continuing from Fig 5 in the Main Text.* FTIR of the N-O stretching region of NO$^+$/H-SSZ-13 system before reaction with ammonia, and after reaction with ammonia (at room temperature), and after pulling high vacuum at 100 °C for 15 minutes.

Figs. S4. *Continuing FTIR experiments after the ones performed in Fig 2A.* After reaction between NO$^+$/H-BEA with ^{15}NH$_3$, the sample was vacuumed at room temperature and new baseline was collected (gray spectrum). 2 Torr NO + 0.7 Torr O$_2$ were then reacted with the sample: the resulting spectra (green and blue) show that because NH$_3$ occupied Bronsted acid sites of zeolite with the formation of NH$_4$-Zeolite (ammonia is strongly adsorbed and cannot be desorbed at room temperature even to a small extent), only extremely small amounts of NO$^+$ can be formed (intensities barely above the noise level).
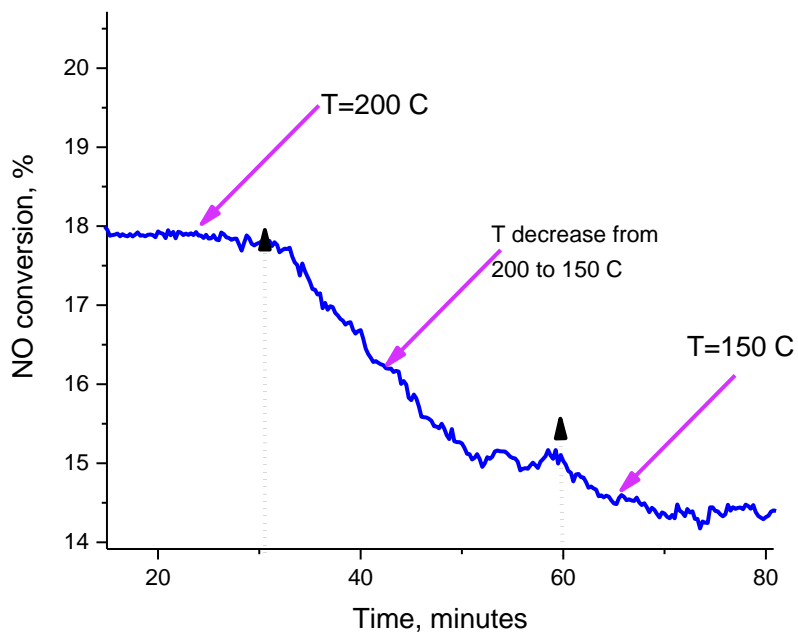
Figs. S5. NO conversion (%) vs time-on-stream for H-BEA Si/Al ~ 15 sample under dry conditions (conditions specified in experimental section).
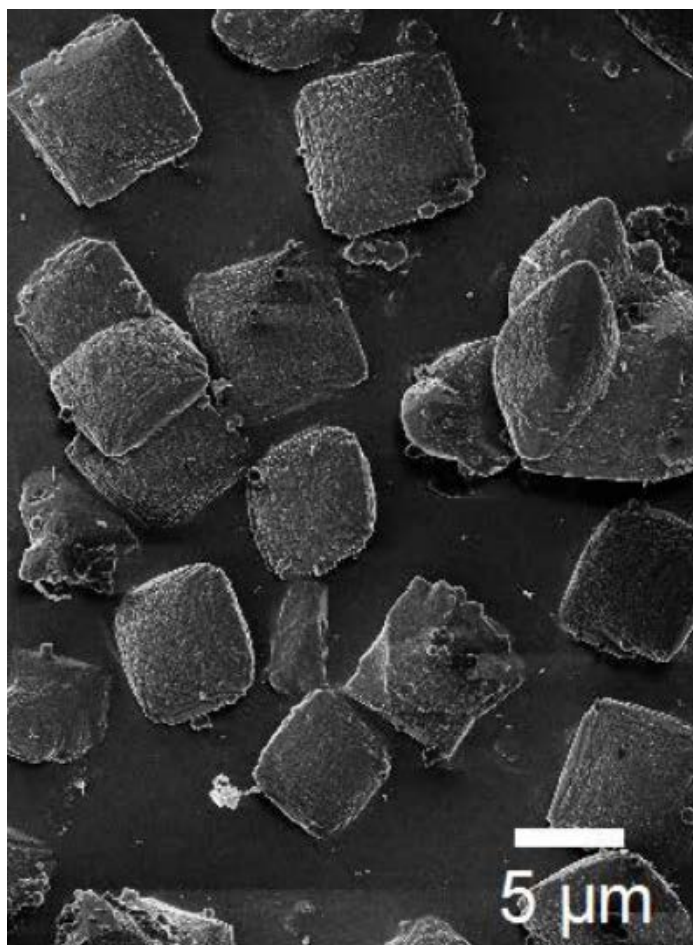
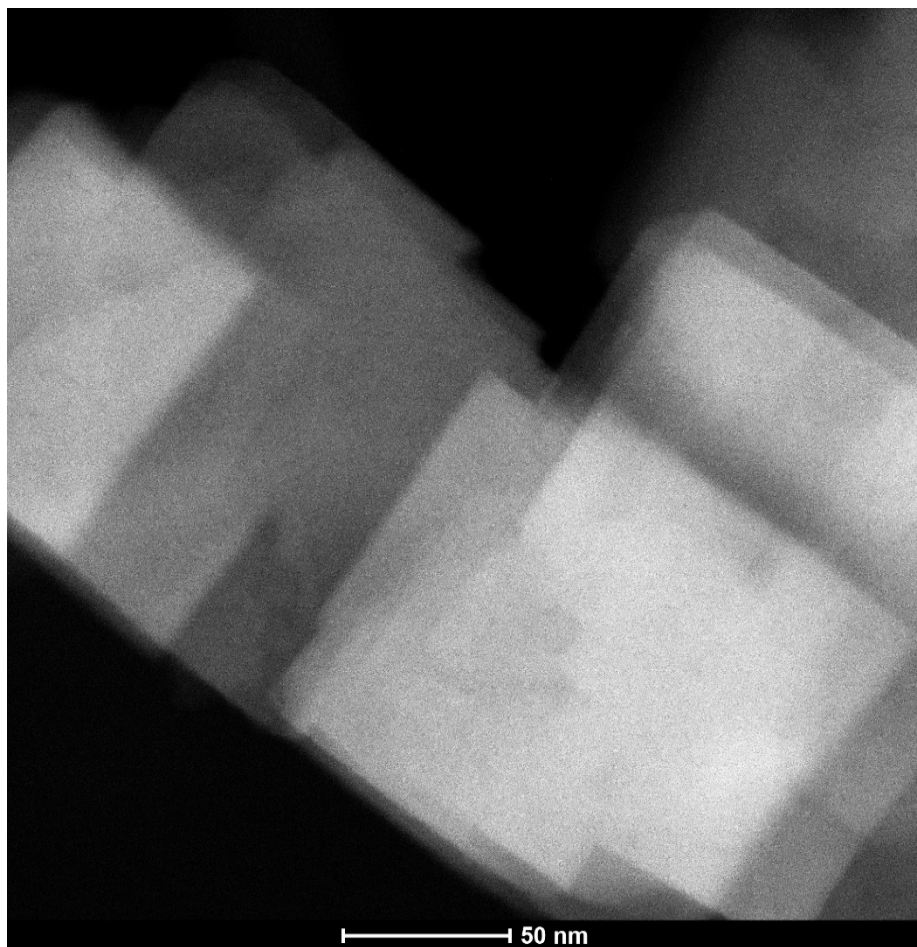Fig. S6. Typical Helium Ion Microscopy (HIM) image of H-BEA crystals with Si/Al ~ 15.

Fig. S7. Typical HAADF-STEM images of SSZ-13 crystals.

5